ISBN: 978-3-95450-233-2 ISSN: 2673-5504 doi:10.18429/JACoW-SRF2021-THPCAV014

DEVELOPMENT OF HIGH-Q TREATMENTS FOR PIP-II PROTOTYPE CAVITIES AT LASA-INFN

M.Bertucci*, A. Bosotti, A. D'Ambros, A. T. Grimaldi, P. Michelato,
L. Monaco, C. Pagani [1], R. Paparella, D. Sertore, INFN-LASA, Segrate (MI), Italy
A. Gresele, M. Rizzi, A. Torri, Zanon Research & Innovation, Schio (VI), Italy
[1] also at Università degli Studi di Milano, Milano (MI), Italy

Abstract

INFN-LASA is currently involved in the production of PIP-II low-beta cavity prototypes. The main challenge of this activity is to develop a state-of-the art surface treatment recipe on such cavity geometry, to achieve the high-Q target required for cavity operation in the linac. This paper reports the status of cavity treatments development and the first cold test results of a single-cell cavity. This cavity has undergone a baseline treatment based on Electropolishing as bulk removal step. Being this test successful, a strategy for pushing the cavities towards higher performances is here proposed.

INTRODUCTION

INFN-LASA joined the international effort for the PIP-II project in Fermilab and is appointed to build 40 650 MHz $\beta = 0.61$ superconducting cavities that will constitute the low-beta section of the Linac. Specifications for cavity operation in the machine are $E_{acc} = 16.9\,\mathrm{MV\,m^{-1}}$ with a $Q_0 \geq 2.4 \cdot 10^{10}$. Electropolishing (EP) was chosen for the upcoming production of PIP-II cavities, so to avoid the Q-slope behavior typical of BCP-treated cavites which would limit the cavity performance below the machine target. This is one of the key challenges of the PIP-II SRF cavity production, and in particular for the low-beta section, where the extremely compressed cavity geometry complicates further the surface processing steps.

To this aim, seven prototype cavities were produced, with both single and multi-cell geometry. Parts of them are shared with Fermilab in sake of a joint development effort on many technical issues. A single cell (B61S_EZ_002) and a multicell (B61_EZ_002) cavity are serving the main purpose of developing and optimizing the treatment recipe. This activity is currently carried out by the SRF group of INFN-LASA.

Cavity prototype production is currently ongoing at the company Zanon Research & Innovation Srl. This activity began with the refurbishment of the EP facility so to host the PIP-II cavities and with the optimization of the treatment parameters on the different cavity shape and geometry. This was done by means of several short EP treatments which were carried out on the single-cell prototype cavity B61S_EZ_002, until the outcome resulted satisfying in terms of surface smoothness, removal rate and iris/equator removal ratio [1]. Being this optimization phase successfully completed, the single cell cavity was ready to undergo the complete baseline treatment, employing a E-XFEL-like recipe [2]. Once the baseline treatment is validated by the results of cavity cold test, the same recipe is expected to be used on a multicell prototype cavity, but with the introduction of a high-Q surface treatment which will allow to reach the PIP-II target.

SINGLE CELL CAVITY SURFACE TREATMENT

The baseline surface treatment employed on the PIP-II single cell prototype cavity B61S_EZ_002 served the purpose of qualifying the surface processing facilities and is based on the same recipe used for the series production of EXFEL 1.3 GHz cavities, with the only variation of cold EP as final surface treatment. The goal of Cold EP is to obtain a smoother surface and a more uniform removal over the cavity [3]. A mirror-finish surface condition is essential for obtaining an high Q-value at the operating gradient, because a rough surface would introduce non-linear losses increasing cavity power dissipation at higher fields [4].

The main steps of the PIP-II baseline recipe are:

- 150 µm bulk EP, in two separate steps of 75 µm each.
- 800 °C heat treatment for 2 hours in ultra high vacuum (UHV) conditions.
- 25 µm final Cold EP.
- High pressure rinsing (HPR) for 12 hours with ultra pure water (UPW).
- 120 °C 48 h low temperature baking.

After each step, the cavity was HPR-rinsed for 2 hours, weighted and dried. A new design for the HPR nozzle head was developed by INFN-LASA so to improve the effectiveness of the rinsing operation on the PIP-II low-β cavity geometry. A RF check was done after every treatment step so to monitor the frequency response. Optical inspection is performed after the Electron Beam Welding and after the bulk EP treatment.

Bulk EP

The bulk EP overall target removal was 150 µm, to be performed in two separate steps of 75 µm each. The optimization campaign resulted in the following choices for the treatment parameters and of the plant layout:

- A 30 mm diameter Aluminum cathode was employed, with a cylindrical enlargement installed at the equator position. This allowed to remarkably increase the removal at the equator. Fresh acid flows in the cavity through a hole at equator position with a 1 L min^{-1}

* michele.bertucci@mi.infn.it

ISBN: 978-3-95450-233-2 ISSN: 2673-5504 doi:10.18429/JACoW-SRF2021-THPCAV014

throughput. The cathode was shielded with a PTFE tape in correspondence of beam tubes, so to locally reduce the removal.

- A $V = 17$ V voltage was employed, yielding a 48 A average current and a 0.14 µm min^{-1} removal rate.
- The temperature set-point of 20–21°C for the average reading of cavity thermocouples was chosen. When this value was exceeded, the acid chiller turned on. An external water chiller was activated if temperature on beam tube went above 25 °C.

The treatment behavior was monitored online by the reading of current and of the several thermocouples installed on cavity surface. The average removal rate can be instantaneously calculated from the measurement of current by means of the formula:

$$r[\mu\text{m min}^{-1}] = 0.123 \cdot \frac{i[\text{A}]}{S[\text{dm}^2]}\,, \qquad (1)$$

where i is the current and S is cavity internal surface. An apparatus based on Ultrasound (US) transducers allows the continuous acquisition of thickness [5]. During this treatment, 3 probes were placed on cavity iris, wall and equator, respectively. The data registration during the first EP step is shown in Fig. 1. The overall removal and removal rates of the 2 steps – as extrapolated from experimental data – are shown in Table 1.

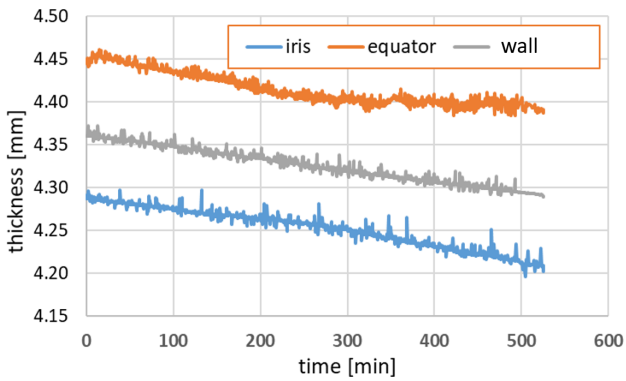

Figure 1: US thickness registration from cavity iris, equator and wall for the first 75 µm EP substep.

The removal rates as extimated by the US reading are consistent with the average values obtained by cavity weighting and by total removed charge, which are both 0.14 µm min^{-1}.

Table 1: Total Thickness Removal and Removal Rates at Different Points of the Cavity Surface

Step	Removal Parameter	Iris	Wall	Equator
1	rate [µm min^{-1}]	0.15	0.13	0.12
	removal [µm]	82	71	61
2	rate [µm min^{-1}]	0.14	0.12	0.11
	removal [µm]	76	70	59

Cold EP

After the 800 °C annealing in a UHV oven, the cavity underwent the final surface treatment. The Cold EP consisted of two separate phases: a first "warm" phase exploiting the same treatment parameters of the bulk EP, with a 20–21°C temperature set-point for acid inlet chilling. An overall 15 µm average removal on cavity surface was achieved in this condition. Then, the voltage was turned off and the acid in the barrel was cooled down to 7–8°C. In this "cold" phase a lower setpoint for acid chilling was set (max 15 °C on cavity cell, max 18 °C on beam tubes). The overall removal in this conditions was 10 µm. The temperature and current trend of the cold EP treatment is shown in Fig. 2. The colder acid temperature resulted in a significant decrease of current, which dropped from 50 A to around 30 A. In its turn, removal rate went from 0.14 µm min^{-1} to 0.08 µm min^{-1}.

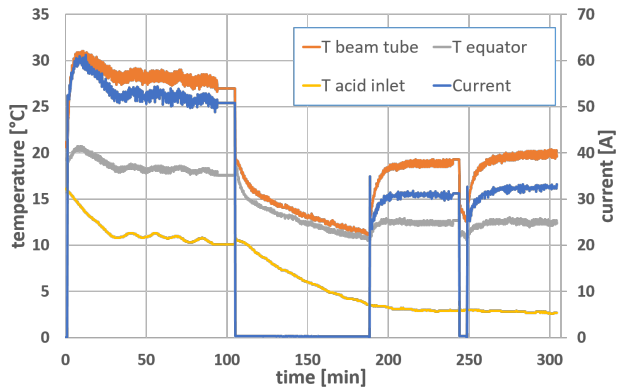

Figure 2: Temperature and current trend during the Cold EP treatment.

SINGLE CELL CAVITY TEST

After the complete surface treatment, cavity B61S_EZ_002 was tested at INFN-LASA vertical test facility. The cryostat allows to reach temperatures as low as 1.5 K. The cavity test stand is equipped with diagnostics for the detection of quench events (second sound, fast thermometry) and field emission (photodiodes inside cryostat, external proportional counter and NaI scintillator) [6].

A fluxgate cryogenic sensor was placed on the cavity surface to measure magnetic flux expulsion across the critical temperature (9.2 K). Cooldown rate was less than 1 K min^{-1} so the residual magnetic field (max. 8 mG in the cryostat inner volume) is expected to be completely trapped. Indeed, no magnetic flux variation was measured by the fluxgate. Assuming a trapped flux sensitivity of 0.3 nΩ mG^{-1} [7] for baked niobium at 650 MHz, one should then expect a $R_{fl} =$ 2.4 nΩ contribution to residual surface resistance.

Cavity surface resistance was measured during the cooldown. The R_s vs T data were fitted with SUPERFIT 2.0 code [8], which employs Halbritter quasi-exponential formula for the BCS resistance. The fit results for reduced

ISBN: 978-3-95450-233-2 ISSN: 2673-5504 doi:10.18429/JACoW-SRF2021-THPCAV014

band gap, electron mean free path and residual resistance are $\frac{\Delta}{k_B T} = 1.85$, $l_e = 26\,\text{nm}$ and $R_{res} = 4.35\,\text{n}\Omega$, respectively.

The results of the vertical tests performed at INFN-LASA lab are shown in Fig. 3. In the first test at 2 K the cavity reached 30 MV m^{-1}, displaying a high-field Q-slope. This behavior is related to field emission, which converts part of the incident power into electron dark current. High-field RF conditioning was attempted so to mitigate the level of field emission. The conditioning was interrupted after 40 minutes due to limitations of the cryogenic plant. The test was then repeated, and a slight degradation of Q_0 at high fields was noticed, together with the increase of radiation level of an order of magnitude. Even the onset of FE displaced from 17 MV m^{-1} to 12 MV m^{-1}. However, radiation level was of the order of 10 µSv h^{-1} near the target gradient of 16.9 MV m^{-1}.

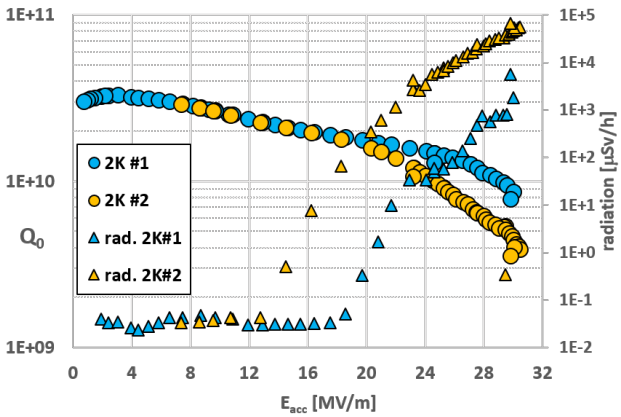

Figure 3: Q_0 vs E_{acc} before and after high-field RF processing. The radiation level is also shown on the secondary axis.

The photodiodes readout during the first power test is shown in Fig. 4. Photodiodes #1 and #2 are installed near the upper cavity iris, at opposite angles, photodiodes #3 and #4 are placed nearby the lower cavity iris, at the same angular position. All the signals start to rise at 17 MV m^{-1} but at different voltage levels. The lower photodiodes detect at first a higher level of radiation, but upper sensors rapidly regain the ground eventually overtaking the lower ones at 27 MV m^{-1}. this behavior, which is still under investigation, can be related to the change of emitter topology, which could also be the cause of the Q-degradation in the second test.

From the performance point of view, $Q_0 = 2 \cdot 10^{10}$ at $E_{acc} = 16.9\,\text{MV m}^{-1}$, which corresponds to $R_s = 5.6\,\text{n}\Omega$. It must be stressed that the test was done in a slow cooldown regime so that one could easily get rid of a $R_{fl} = 2.4\,\text{n}\Omega$ contribution to residual resistance by means of a proper magnetic hygiene protocol. Assuming a perfect flux expulsion, or canceling the external magnetic field by compensation coils, one can calculate the theoretical Q_0 by subtracting R_{fl} from the experimental surface resistance R_s. Thus, a $Q_0 = \frac{G}{R_s - R_{fl}} = 2.5 \cdot 10^{10}$ can be virtually obtained. An upgrade of the vertical test facility (magnetic shielding and cryogenic system) is foreseen for the next future and will

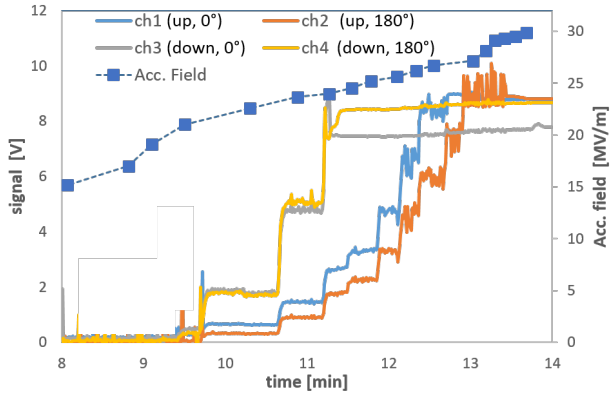

Figure 4: Photodiode readout during the cavity power test.

allow to decrease the magnetic field contribution to residual resistance and so to reach higher Q-values.

MULTI-CELL CAVITY SURFACE TREATMENT

The high-Q treatment for the multi-cell prototype cavity was chosen according to some general considerations. The Nitrogen doping recipe, well consolidated during the LCLS-II series production, requires an high temperature treatment (above 900 °C) so to achieve full material re-crystallization and then improve the magnetic flux expulsion characteristics. But it is also well known that increasing the annealing temperature will lower the niobium yield strength. This in turn can be detrimental for cavity mechanical stability, especially for the case of PIP-II $\beta = 0.61$ geometry. Taking all this into account, the so called mid-temperature bake was chosen instead. This recipe has been already successfully employed [9, 10] with outstanding performances in terms of Q_0 values at low and medium fields, so it is expected to drive the cavity above the PIP-II target at the operating gradient, even without the need of a $T > 900\,°\text{C}$ annealing.

The main steps of the recipe are:

- 150 µm bulk EP, with the last 5 µm performed at cold.
- 800 °C heat treatment for 2 hours in UHV conditions.
- 5 µm final Cold EP.
- 300 °C heat treatment for 3 hours in UHV conditions.
- High pressure rinsing (HPR) for 12 hours with ultra pure water (UPW).

Similarly to what occurs in the standard 120 °C bake, it is thought that the beneficial effect of mid-temperature bake is related to the redistribution of oxygen content in the subsurface layer. Such oxygen diffusion inhibits hydrides segregation, which would introduce additional losses in the RF penetration depth due to the proximity effect [11]. This means that no additional surface removal has to be done after the mid-temperature bake, otherwise the oxygen profile will be completely cancelled. In its turn, this implies that particular care must be taken to preserve surface cleanliness during the last steps. For instance, any residual gas in the furnace would propagate inside the niobium bulk with a

ISBN: 978-3-95450-233-2 ISSN: 2673-5504 doi:10.18429/JACoW-SRF2021-THPCAV014

diffusion length over time t given by $d = \sqrt{D(T)t}$, where the temperature-dependent diffusivity can be expressed by the Arrhenius equation: $D(T) = D_0 \cdot \exp(-E_A/RT)$, where D_0 is the maximal diffusion coefficient, E_A the molar activation energy, T the temperature in K and R the gas constant. Considering for instance the case of carbon, which is a contamination often encountered during heat treatments [12], employing the values for D_0 and E_A reported in [13] and assuming 3 hours of surface exposure to oven residual gases at 300 °C, one obtains a diffusion length $d = 9.3$ nm. Even though this value is by a great deal smaller than typical diffusion lengths at $T = 800$ °C (which are on the µm scale), is on the same scale of London penetration depth (39 nm). Such contamination is expected to noticeably degrade the cavity performances. In order to protect the cavity inner surface from furnace contamination during the mid-temperature bake, protective caps made from niobium foils will be placed to cover the cavity flanges openings [14].

Main EP

Being the EP treatment of the single-cell cavity successful, the same method of operation was followed for the multi-cell cavity prototype, scaling all arameters to the 5-cell case:

- 5 Aluminum enlargements were installed in correspondence of the cells.
- Acid exits from cathode through 5 holes in correspondence of equators.
- The external water chiller was adapted so to pour continuosly cold water on cavity irises and beam tubes.
- Overall acid throughput is increased so to yield at least 1 L min^{-1} for cell.

Figure 5 shows the cavity B61_EZ_002 installed in the EP plant. A first EP trial with a 30 µm target was performed so to check if the same parameters used for the single cell cavity prototype would yield the same outcome in terms of surface smoothness, removal rate and iris-equator removal ratio. This trial was successful, so that the the full EP treatment was then carried out with the same parameters.

Figure 5: Cavity B61_EZ_002 installed on the EP plant.

The data registration for the last 500 minutes of the treatment is shown in Fig. 6. The first 300 minutes represents the last part of the ordinary "warm" EP. Inlet acid temperature is 11 °C which corresponds to an average current of 180 A. Then, acid in the barrel is cooled down below 5 °C so to remove the last 5 µm in the "cold" regime. Accordingly, current dropped down to an average value of 90 A. In both warm and cold regimes, a good temperature uniformity on cavity surface is obtained thanks to the action of external water chiller, as demonstrated by the temperature reading on iris and equator shown in Fig. 6.

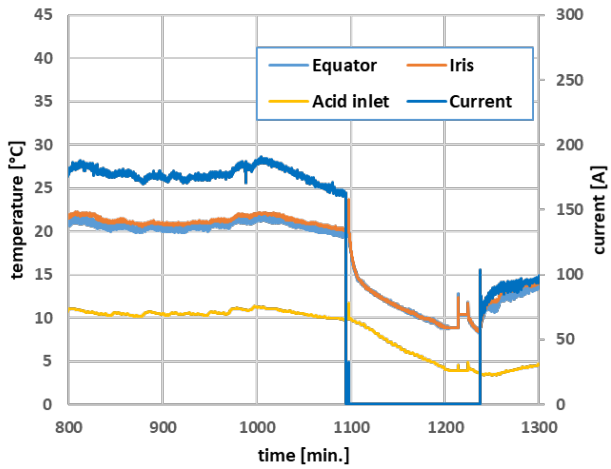

Figure 6: Data from the last 500 min of first EP step: acid inlet, iris and equator temperature, and current.

Table 1 summarizes current and removal rates, as calculated by eq. (1), for the single cell and multi-cell cavity prototypes, and in the 2 different EP regimes. The data of current is defined as the average over a significant time interval where the process reached a steady state. There is a marginal reduction of the removal rate in the multi-cell case with respect to the single cell, probably due to the lower inlet acid temperature. In the cold EP, removal rate is reduced by nearly a factor 2 with respect to the warm case.

Table 2: Removal Rates for Single and Multi-Cell Prototypes in the Warm and Cold EP Regimes

Regime	Parameter	Single Cell	Multi-Cell
warm	current [A]	50	180
	rem. rate [µm min^{-1}]	0.14	0.13
cold	current [A]	30	90
	rem. rate [µm min^{-1}]	0.08	0.07

The local removal in several points of interest of cavity surface is measured by means of an US probe. The results are depicted in Fig. 7. As it is evident from the graph, the removal at all equator sites is very close to the overall average removal of 150 µm, while on cavity beam tubes the removal is around 200 µm. We can therefore conclude that the EP treatment was effective in removing the damaged layer at

ISBN: 978-3-95450-233-2 ISSN: 2673-5504 doi:10.18429/JACoW-SRF2021-THPCAV014

the equator sites, thanks to the enhancement in current introduced by the Aluminum enlargements.

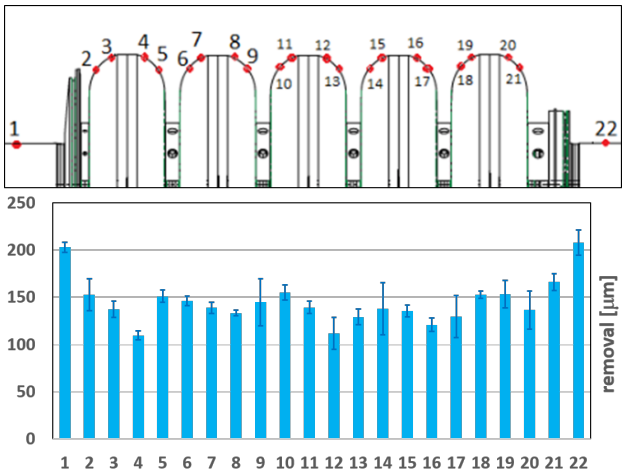

Figure 7: Local removal in several points of interest of cavity surface, as measured by US probe.

CONCLUSIONS

A 650 MHz $\beta = 0.61$ single cell prototype for PIP-II underwent a complete surface treatment. A good surface finishing was achieved and the desired iris over equator removal rate was reached. Cavity performances are close to the target Q_0 at the nominal gradient, although the residual magnetic field in the cryostat is completely trapped due to low cooldown rate at the transition temperature. Assuming no contribution of external magnetic field to surface resistance, such baseline recipe would be enough to meet the PIP-II specifications.

Given this, we proceeded with the high-Q treatment of B61_EZ_002 multi-cell cavity prototype. Our goal is to exploit a recipe which does not require any high temperature annealing to recover the magnetic expulsion properties of the material. So the cavity treatment cycle was based on the so called mid-temperature bake, which is a promising alternative to Nitrogen doping when one aims to reach a high-Q target at a moderate operating gradient, as it is the case of the low β section of PIP-II Linac.

REFERENCES

[1] M. Bertucci *et al.*, "Electropolishing of PIP-II Low Beta Cavity Prototypes", in *Proc. 19th Int. Conf. RF Superconductivity (SRF'19)*, Dresden, Germany, Jun.-Jul. 2019, pp. 194–198. doi:10.18429/JACoW-SRF2019-MOP057

[2] W. Singer, *et al.*, "Production of superconducting 1.3-GHz cavities for the European X-ray Free Electron Laser", *Phys. Rev. Accel. Beams*, vol. 19, p. 092001, 2016. doi:10.1103/PhysRevAccelBeams.19.092001

[3] F. Furuta, D. Bice, A. C. Crawford, and T. Ring, "Fermilab EP Facility Improvement", in *Proc. 19th Int. Conf. RF Superconductivity (SRF'19)*, Dresden, Germany, Jun.-Jul. 2019, pp. 453–455. doi:10.18429/JACoW-SRF2019-TUP022

[4] K. Saito, "Surface Smoothness for High Gradient Niobium SC RF Cavities", in *11th Workshop on RF Superconductivity (SRF' 03)*, Lübeck/Travemünde, Germany, Sep 2003, paper THP15, pp. 637–640.

[5] M. Bertucci *et al.*, "An apparatus for the continuous measurement of thickness during the electropolishing of superconducting cavities", in *Rev. Sci. Instrum*, vol. 92, p. 023307, 2021. doi:10.1063/RevSciInstrum.92.2.023307

[6] M. Bertucci *et al.*, "Quench and Field Emission Diagnostics for the ESS Medium-Beta Prototypes Vertical Tests at LASA", in *Proc. 8th Int. Particle Accelerator Conf. (IPAC'17)*, Copenhagen, Denmark, May 2017, pp. 1007–1010. doi:10.18429/JACoW-IPAC2017-MOPVA061

[7] M. Checchin *et al.*, "Frequency Dependence of the Trapped Flux Sensitivity in SRF Cavities", *Appl. Phys. Lett.*, vol. 112, p. 072601, 2017. doi:10.1063/1.5016525

[8] G. Ciovati, "SUPERFIT: a Computer Code to fit Surface Resistance and Penetration Depth of a Superconductor", Tech Rep. TN–003, Jlab, 2003.

[9] S. Posen, A. Romanenko, A. Grassellino, O.S. Melnychuk, and D.A. Sergatskov, "Ultralow Surface Resistance via Vacuum Heat Treatment of Superconducting Radio-Frequency Cavities"in *Phys. Rev. Applied*, vol. 13, p. 014024, 2020. doi:10.1103/PhysRevApplied.13.014024

[10] F. He *et al.*, "Medium-temperature furnace bake of Superconducting Radio-Frequency cavities at IHEP", arXiv:2012.04817

[11] A. Romanenko, F. Barkov, L. Cooley, and A. Grassellino, "Proximity breakdown of hydrides in superconducting niobium cavities", in *Supercond. Sci. Technol.*, vol. 26, p. 014024, 2012. doi:10.1088/0953-2048/26/3/035003

[12] M. Wenskat *et al.*, "Nitrogen infusion R&D at DESY a case study on cavity cut-outs", in *Supercond. Sci.Technol.*, vol. 33, p. 115017, 2020. doi:10.1088/1361-6668/abb58c

[13] J. Imai, O. taguchi, G. Tiwai, and Y. Iijima, "Diffusion of Carbon in Niobium and Molybdenum"in *Mater. Trans*, **55** (2014), pp 1786–1791. doi:10.2320/matertrans.M2014277

[14] A. Grassellino *et al.*, "Unprecedented quality factors at accelerating gradients up to 45 MV m^{-1} in niobium superconducting resonators via low temperature nitrogen infusion", in *Supercond. Sci.Technol.*, vol. 30, p. 094004, 2017. doi:10.1088/1361-6668/aa7afe